Some Evolutionary Relationships of the Primary Biological Catalysts Glutamine Synthetase and RuBisCO

D. EISENBERG, R.J. ALMASSY, C.A. JANSON, M.S. CHAPMAN, S.W. SUH, D. CASCIO, AND W.W. SMITH
Molecular Biology Institute and the Department of Chemistry and Biochemistry, University of California, Los Angeles, California 90024

The polypeptide folds of two primary biological catalysts have been determined by X-ray crystallography. One is glutamine synthetase (GS) from *Salmonella typhimurium*, which catalyzes the entry of nitrogen into metabolism, and the other is ribulose bisphosphate carboxylase/oxygenase (RuBisCO) from tobacco, which catalyzes the entry of carbon into metabolism. Both are oligomeric structures having complicated patterns of interdomain and intersubunit contacts.

In this paper we consider three questions: (1) What are the patterns of folding of polypeptide chains in GS and RuBisCO, and how do the folded domains interact in the oligomeric enzyme? (2) Which features of the folding patterns are conserved in distantly related species and which are changed? and (3) What do the patterns of conservation and change tell us about the evolution of these catalytic functions?

Both GS and RuBisCO are primary biological catalysts in the sense that they catalyze the first steps at which nitrogen and carbon, respectively, are brought into cellular metabolism. GS (Ginsburg 1972; Ginsburg and Stadtman 1973) brings nitrogen into metabolism by condensing ammonia with glutamate, with the aid of ATP, to form glutamine:

$$\text{L-Glutamate} + NH_4^+ + ATP \longrightarrow \text{L-Glutamine} + ADP + P_i$$

Glutamine is in turn a source of nitrogen in the biosynthesis of numerous nitrogen-containing metabolites, including amino acids, nucleotides, and amino sugars. Some nine of these end products of glutamine metabolism are feedback inhibitors of bacterial GS. GS in enteric bacteria is also regulated by covalent modification of a tyrosine residue by adenylylation (Shapiro et al. 1967). GS is adenylylated by a multienzyme cascade system in response to high levels of glutamine, and this modified GS has heightened sensitivity to the feedback inhibitors. In higher cells, GS also plays a central metabolic role. In plants, for example, GS assimilates ammonia produced by nitrogen fixation in roots and also assimilates ammonia released by photorespiration in leaves.

The three-dimensional structure of the 12-subunit GS from *S. typhimurium* has been determined at 3.5 Å (Almassy et al. 1986) and is described briefly below. A remarkable feature of the enzyme structure is that the catalytic site is formed from portions of two polypeptide chains, at the subunit interface. This finding in itself suggests that bacterial GS is not a "primitive" enzyme, in that primitive GS enzymes presumably contained a catalytic site completely within one polypeptide chain.

The question of how the GS function evolved deepens when we consider that plant and animal GS molecules contain 8 identical subunits (Meister 1974), rather than 12 as in bacteria. In this paper, we present a speculative hypothesis on the relationship of the structure of the plant GS with 8 subunits to the bacterial molecule with 12 subunits. It is based in part on the observation that some segments of the amino acid sequences of plant and bacterial GS molecules are more strongly conserved than others. The stronger conservation tends to be in segments that form features of the active site. We show that features of the active sites can be conserved in an octameric GS molecule, provided that the symmetry of the octamer is lower than that of an ideally symmetric molecule. A lower symmetry octamer is consistent with some measurements on stoichiometry of binding.

RuBisCO catalyzes the first step of the Calvin cycle of photosynthesis (Miziorko and Lorimer 1983; Ellis and Gray 1986), in which carbon is brought into cellular metabolism in the form of carbon dioxide:

$$CO_2 + \text{Ribulose-1,5-bisphosphate} + H_2O \longrightarrow 2\ \text{3-Phosphoglycerate}$$

RuBisCO also catalyzes the oxidation of ribulose bisphosphate in the first step of photorespiration.

The RuBisCO in plants has the subunit stoichiometry L_8S_8 (Baker et al. 1975), in which L is the large polypeptide chain (M_r 53,000) containing the catalytic residues and S is the small subunit (M_r 15,000). Recently, we have determined a moderate resolution structure for RuBisCO from tobacco (Chapman et al. 1987). It reveals that the catalytic site, like that of GS, is at the interface of two polypeptide chains. A portion of the molecule, containing just two L chains, resembles the structure of the L_2 RuBisCO from the photosynthetic bacterium *Rhodospirillum rubrum* (Schneider et al. 1986). Thus the tertiary structures of *R. rubrum* and plant RuBisCOs are similar for the large subunit polypeptide common to both enzymes, although the quaternary structures are different.

METHODS

X-ray crystallographic methods were used to determine the three-dimensional structures of GS to 3.5 Å resolution and of RuBisCO to 3.0 Å resolution. Some details have been reported by Almassy et al. (1986) and Chapman et al. (1987); additional information on structure determination will be presented elsewhere. Atomic models for both have been built and refined partially to crystallographic R factors of about 0.35. Refinement is continuing for both models, and it is anticipated that the preliminary structures reported here will change in details.

Alignment of the GS amino acid sequence from *S. typhimurium* (Janson et al. 1986) to that of GS from alfalfa (Tischer et al. 1986) was achieved with the University of Wisconsin Genetics Computer Group software package, mainly with the program BESTFIT, using a gap weight of 3.0 and a length weight of 0.1.

RESULTS

Structure of GS from *S. typhimurium*

In bacterial GS, the 12 subunits are arranged with 622 symmetry, just as the carbon atoms of two face-to-face benzene rings. Each subunit contains 468 amino acid residues and two metal ions at the active site. In Figure 1, one layer of 6 subunits is viewed down the 6-fold molecular axis; for clarity the layer below is omitted. In this paper, we are concerned mainly with the interaction of adjacent subunits within one such layer.

Each subunit has two folding domains (Fig. 1). The N domain is formed from the 103 amino-terminal residues, and is mainly a five-strand β sheet. However, this domain contains two α helices: it starts with a 12-residue helix and also contains a short 6-residue helix starting at amino acid 40. The C domain is much larger (residues 104–468). It contains 11 major α helices, and a β sheet with six antiparallel strands. This β sheet forms part of a cylindrical active site at the interface of two subunits within a ring. The rest of the cylinder is formed by two β strands from the neighboring subunit. These two strands are in the N domain; they are residues 44–52 and 59–70, bracketing a loop that contains Trp-57. This antiparallel, eight-strand cylinder is identified in the electron density as the active site both from the two metal ions it contains, and from a difference Fourier map showing that the transition-state analog binds within.

The polypeptide fold of a single GS subunit is shown in Figure 2. The two metal ions are depicted as circles in the active site at the top of the figure. Surrounding these ions are six heavy arrows, representing the six prominent β strands of the C domain. The other two β strands forming the active-site cylinder are at the bottom of the figure, with the position of Trp-57 marked at the bottom of the two strands. This two-strand segment of the structure is called the Trp-57 loop.

In summary, the six active sites within one ring of the GS molecule are between adjacent subunits. The major portion of the active site, including six antiparallel extended strands and eight metal ligands, is donated by the C domain of one subunit; the minor portion, including two β strands, is donated by the N domain of the neighboring subunit.

Relationship between Bacterial and Plant GS Amino Acid Sequences

Amino acid sequences have been inferred from gene sequences for GS from alfalfa (Tischer et al. 1986) and Chinese hamster (Hayward et al. 1986), as well as from *Anabaena* (Tumer et al. 1983), *S. typhimurium* (Janson et al. 1986), and *E. coli* (Colombo and Villafranca 1986). The sequences from alfalfa and Chinese hamster can be readily aligned with over 50% of paired residues being identical (Tischer et al. 1986), a level of similarity that suggests very similar protein folds (Sweet and Eisenberg 1983). Similarly, the sequences from *Anabaena*, *S. typhimurium*, and *E. coli* can be readily aligned (Janson et al. 1986). In contrast, the similarity between the GS amino acid sequences of *S. typhimurium* (or the other bacterial GS) and of higher cells is much smaller, but not insignificant, as is shown in Figure 3. There are four segments in the paired sequences that show strong similarity.

Where in the known three-dimensional structure of bacterial GS do the segments of strong similarity fall? One of these segments includes residues 49–67 in *S. typhimurium*. This segment is the loop containing Trp-57, which can be seen at the bottom of Figure 2. By comparison with Figure 1, it is possible to see that this loop is part of the active site of the adjacent subunit. The second strongly conserved segment extends from

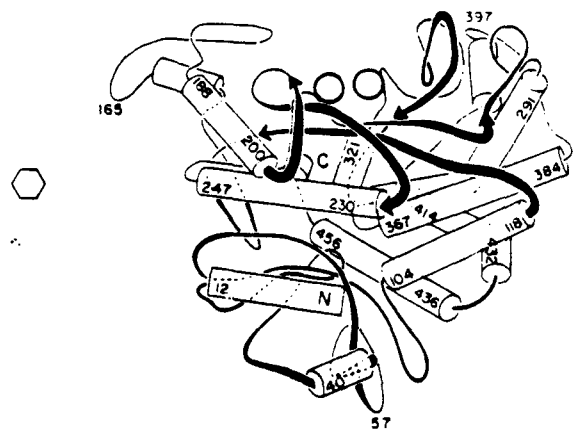

Figure 2. A schematic drawing of the polypeptide chain of one subunit of GS from *S. typhimurium*. (Reprinted, with permission from Almassy et al. 1986.) This subunit corresponds to the one on the right center of Fig. 1. The metal ions are indicated by two circles in the upper center, and the 6-fold axis by the hexagon on the left. Cylinders represent α helices; 6 heavy arrows, prominent β strands surrounding the metals. The amino-terminal folding domain (residues 1–103) is at the bottom. The central loop is at the upper left. The β loop is the U just below the helical end marked 247. (Reprinted, with permission, from Almassy et al. 1986.)

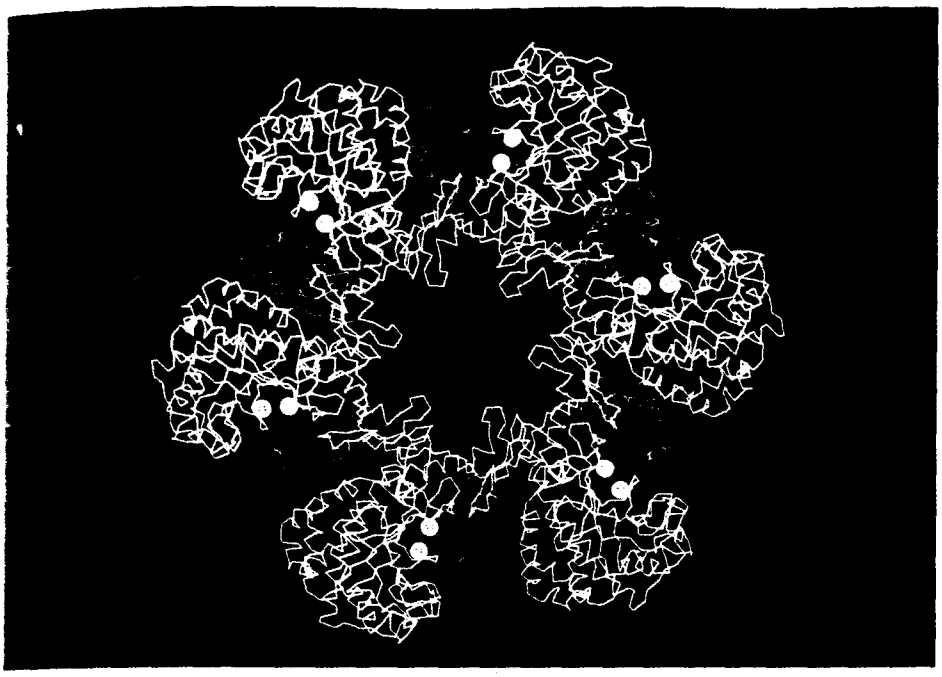

Figure 1. GS from *S. typhimurium* projected down the 6-fold molecular axis. The six subunits of the upper ring are shown as lines connecting sequential α carbon atoms. The N domains (residues 1–103) are shown in red and the C domains (residues 104–468) in blue. The central cavity, 40 Å in diameter, is filled with solvent, except for the central loops from each subunit, which protrude in about 15 Å. The active sites are cylindrical channels, each holding two Mn^{++} ions, shown as white circles. The N and C domains that meet at each active site are on *different* subunits. The molecule, including side chains, is 143 Å in diameter.

Figure 4. The spatial arrangement of subunits and domains in tobacco RuBisCO. (Reprinted, with permission, from Chapman et al. 1987.) S subunits are in blue, and each L subunit is in a different color. Notice that the amino-terminal domain of the green L subunit sits close to the mouth of the α/β barrel of the red barrel domain. Small helical carboxy-terminal domains of the L subunits are omitted for clarity.

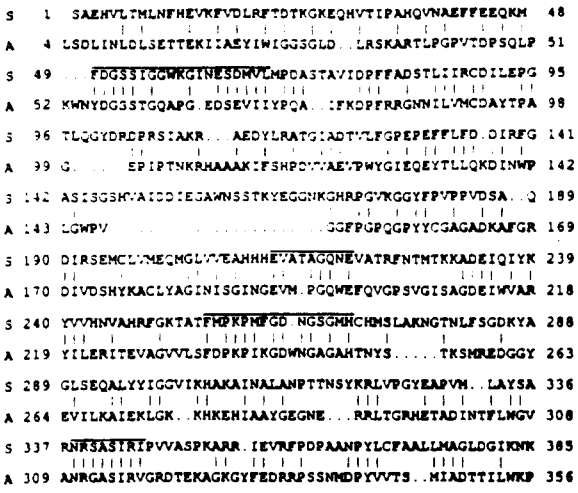

Figure 3. Alignment of amino acid sequences of GS from *S. typhimurium*, labeled S. and from alfalfa, labeled A. Identical or similar residues in the two sequences are indicated by vertical lines. Four strongly conserved segments discussed in the text are indicated by overbars.

residue 212 to 220 in the sequence. In Figure 2 this is a turn and β strand that pass next to the metal ions in the active site. The third conserved segment comprises residues 255–270, another turn and β strand in the active site. A turn and β strand in the active-site cylinder comprise the fourth conserved segment, residues 338-345. In short, all of the strongly conserved segments of sequence between bacterial and alfalfa GS are known in *S. typhimurium* GS to line the active-site cylinder. This suggests that the polypeptide geometries of the active sites of the alfalfa and bacterial enzymes are similar.

In the alignment of Figure 3, a large gap appears in the alfalfa sequence between residues 147 and 148. The segment of the bacterial sequence that aligns in this gap corresponds to two extended loops in the known GS structure. The first of these is the "β loop", which makes contact with the lower layer of 6 subunits. The β loop is visible in Figure 2 as the U-shaped loop just under the end of the helix marked by residue 247. The second loop is the "central loop", which protrudes into the central aqueous cavity of the dodecameric enzyme. This loop is marked by residue 165 in Figure 2. The sequence alignment of Figure 3 suggests that these two loops may be absent in the GS of higher cells.

Structure of RuBisCO from Tobacco

At low resolution, RuBisCO resembles a keg with the axis of the keg being the 4-fold axis of the 16-subunit molecule. The keg is 105 Å along the 4-fold axis and about 132 Å in diameter at its widest point. Along the 4-fold axis there is an open channel, 28 Å wide at the center of the molecule and 6 Å at its narrowest constriction (Chapman et al. 1986).

The arrangement of subunits in tobacco RuBisCO is depicted schematically in Figure 4, where the 4-fold keg axis runs vertically. Clustered around the 4-fold axis at both the top and bottom of the molecule are tetramers of S subunits, shown in blue. Bridging between the two tetramers of S subunits are elongated L subunits, each one a different color in Figure 4. The L subunits have two main folding domains. The amino-terminal (N) domain of about 150 residues is a β-sheet structure with two α helices on the inside, toward the 4-fold axis. The larger domain is an α/β barrel (B) domain, with dimensions and topology very similar to the α/β barrel of triosephosphate isomerase (Banner et al. 1975).

The active site of RuBisCO is at the opening of the α/β barrel onto the solution, as surmised by analogy to other α/β barrel enzymes, and from our preliminary fitting of segments of the amino acid sequence into the electron density. From Figure 4 it can be seen that the active-site region is near the N domain of the adjacent L subunit. Thus RuBisCO, like GS, has its active site at the junction of two domains, which are on different polypeptide chains.

Relationship of Tobacco RuBisCO to *R. rubrum* RuBisCO

In earlier work, we compared the amino acid sequence of the L subunit of tobacco (477 residues) to that of *R. rubrum* (466 residues) (Janson et al. 1984). The method of hydrophobicity correlation was used to assess the probability that the two polypeptide chains are folded in a similar manner. It was found that there is a reasonably high correlation in the hydrophobicities of the pairs of residues in the aligned sequences, suggesting that the two polypeptide chains are folded in the same general way.

This inference, based on comparison of amino acid sequences, has now been confirmed by X-ray diffraction studies of structure. The structure of *R. rubrum* RuBisCO at 3 Å resolution has been reported by Schneider et al. (1986). The polypeptide chain is folded into two main domains, and the L_2 molecule has the same general fold and dimensions as that for one of the four L_2 dimers in the plant L_8S_8 form. The red and green L subunits of Figure 4 contribute one such dimer. Moreover, a 2-fold axis of symmetry relates the two subunits of the *R. rubrum* dimer in nearly the same way that one of the 2-fold axes of the tobacco RuBisCO relates the green and red *L* chains in Figure 4. The S subunits in the L_8S_8 tobacco RuBisCO are not present in *R. rubrum*. It is possible that the tetramers of S subunits in the plant enzyme may function as a scaffold for tetramerizing L_2 dimers of the type found both in *R. rubrum* and tobacco.

DISCUSSION

Possible Relationship of Bacterial and Higher GS Structures

It may be possible to infer some aspects of the structure of GS from higher cells. In this section we argue that the active sites found at the junction of subunits in

bacterial GS are present also in higher GS molecules. This speculation is based in part on the comparison of amino acid sequences made in Figure 3 above, and in part on a comparison of the catalytic and ligand-binding behavior of the two classes of GS.

GS molecules from liver, brain, and plant tissues are somewhat smaller in subunit mass than bacterial GS (M_r = 39,000–50,000 versus 52,000) and have 8 subunits rather than 12 (Tate and Meister 1973). Many of the catalytic and regulatory properties of GS from higher cells are like those from bacteria, but some differ. GS from liver, brain, pea, and *E. coli* all require divalent cations for activity, act on D- as well as L-glutamate, and are inhibited by L-methionine-S-sulfoximine, glycine, alanine, and carbamyl phosphate (Tate et al. 1972). On the other hand, tryptophan, histidine, and glucosamine-6-phosphate inhibit GS from *E. coli* and slightly inhibit GS from pea but do not inhibit GS from liver or brain. GSs from enteric bacteria are regulated by adenylylation, but GSs from *Bacillus subtilis* and higher cells are not. Tate and Meister (1971) summarize the situation as follows: "...the active catalytic sites of these enzymes (and the mechanisms of the reactions catalyzed) are probably quite similar."

Three similarities between the bacterial and higher GSs argue that the protein fold of the higher GS resembles that of the bacterial molecule. The first is the similarity in subunit size. The second is the strong similarity of four segments of the amino acid sequence, discussed above. The third is the similarity in catalytic and regulatory function described in the preceding paragraph. However, with the active site at the interface between two subunits, how can identical subunits be positioned to form both 12mers (bacteria) and octamers (higher cells) and in both cases maintain the active conformation at the subunit interfaces?

In fact, an octamer can be formed from subunit pairs that preserve the intersubunit geometry of the active sites of bacterial GS. However, this packing reduces the symmetry of the octamer to one with half its active-site peptide segments not actually forming active sites. This packing is illustrated by Figure 5, where the top layer of the octamer is depicted as four GS subunits of the bacterial type. Two subunit pairs of the bacterial type are preserved, so that the four subunits form two potent active sites and four impotent half active sites. In this model, a lower layer of four GS subunits is related to the upper layer by two 2-fold axes in the plane of the paper. Thus the symmetry of the octamer is 222, rather than the maximum possible 422.

A consequence of this model is that higher cell GS would be expected to exhibit "half-of-the-sites" activity. In fact, half-of-the-sites binding has been reported for several substrates and effectors. Tate and Meister (1971) found that four moles of methionine sulfoximine bind to octameric rat liver GS and completely inactivate the enzyme. Wedler et al. (1982) found that octameric sheep brain GS binds four moles of Mn^{++} tightly and then four moles more somewhat less tightly. Thus higher GS may demonstrate the half-of-the-sites activity that must be observed in a symmetry 222 octamer that preserves subunit pairs of the type observed in bacterial GS. It should be noted, however, that there could be reasons for half-of-the-sites function other than the diminished symmetry oligomer proposed here. A recent study of the binding of Mn to brain GS is in conflict with earlier work (Maurizi et al. 1986).

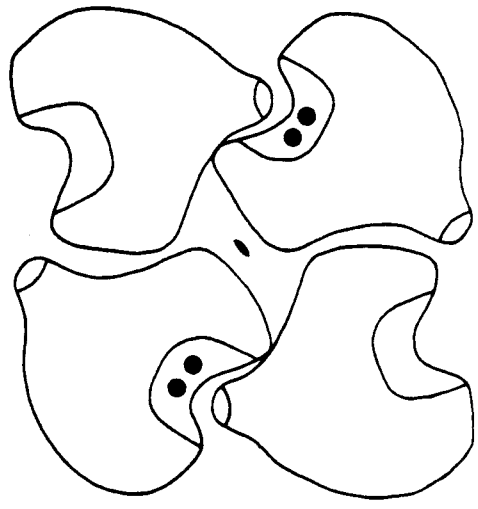

Figure 5. A hypothetical subunit arrangement for GS from higher cells. The enzyme is an octamer, with only the upper layer of four subunits shown. Subunits are arranged in an upper pair and a lower pair, with the two members of each pair having the same spatial relationship as a pair of subunits from bacterial GS (as in Fig. 1). However, the four pairs are arranged with 222 symmetry, rather than 622 symmetry of the six pairs in Fig. 1. The result is that one complete active site is present at the interface of each subunit pair. These complete active sites are indicated by two circles, representing the catalytic metal ions. Each pair also has two vestigial half active sites which could conceivably act as regulatory sites.

The subunit-level model for higher cell GS shown in Figure 5 is also consistent with the loss of the central loop in higher GS suggested by Figure 3. This curious structural feature of *S. typhimurium* GS protrudes into the central solvent channel. It interacts with the active site (see Almassy et al. 1986), but could conceivably interfere with tight association of two subunit pairs. Finally, there is one feature of the model of Figure 5 that is inconsistent with the sequence alignment of Figure 3. It is that lack of any strong homology between the carboxy-terminal amino acid sequences of bacterial and higher cell GS. The carboxyl termini are important for holding together the two layers of bacterial GS, and these interlayer contacts might be expected to be preserved in higher GS, constructed as in the model of Figure 5. Given this lack of homology in the carboxyl termini, as well as the ongoing discussion about binding data mentioned above, the model of Figure 5 must be regarded as highly speculative.

Complexity of the primary biological catalysts. GS and RuBisCO catalyze the primary steps in the assimilation of nitrogen and carbon, respectively. In bacterial systems they might have been expected to have primi-

tive structures. In fact, the structures are very complex: Both structures involve multiple subunits, two main domains in both GS and RuBisCO subunits, and active sites formed from two domains at the junction of subunits. Clearly these primary catalysts have evolved from simpler enzymatic units.

One intriguing question regards the pathway of development from single-domain, single-subunit precursors of these multiple-subunit enzymes containing multiple-domain subunits. The first step might have been multiple-domain formation (i.e., evolution of protomeric chains resembling the GS subunit or the RuBisCO L subunit). Then, the second step would have been oligomerization of these subunits. Alternatively, oligomers of single-domain subunits could have been formed first, followed by development of folding domains within the subunits. From our present knowledge of the structures, neither possibility can be ruled out.

Patterns of evolutionary change and conservation in GS and RuBisCO. In comparing structures of bacterial and higher cell primary catalysts, which features are preserved and which are changed? Quaternary structures are not conserved from one kingdom to another. Bacterial GS contains 12 identical subunits, whereas higher cell GS contains 8. Similarly RuBisCO from the photosynthetic bacterium *R. rubrum* has 2 identical L chains with symmetry 2, and RuBisCO from plants has 8 L and 8 S subunits with symmetry 422. However, within the octamer of L subunits, there are 4 L_2 pairs, each resembling the dimensions of the *R. rubrum* pair (Schneider et al. 1986; Chapman et al. 1987). The variation among species of quaternary structures of enzymes has been noted often before, and a detailed description of comparative RuBisCO quaternary structures has been given by McFadden et al. (1986).

There are indications that tertiary folds of RuBisCO and GS are conserved among kingdoms. The pattern of folding of the L subunit within the tobacco L_8S_8 RuBisCO (Chapman et al., 1987) is at least qualitatively similar to that of *R. rubrum* RuBisCO (Schneider et al. 1986). Both chains have two domains, each domain is similar to its counterpart in the other protein, and the geometry of connection of the two domains is similar in the two molecules.

In GS there are also indications that the tertiary folds of bacterial and higher cell GS are at least partially conserved. This indication is from the conservation of residues in active-site peptides. The observation that one of these conserved regions lies in the N domain of bacterial GS and the other three lie in the C domain suggests that higher cell GS, like bacterial GS, has a two-domain structure.

In short, at our present state of knowledge it appears that the tertiary structures and domain structure of GS and RuBisCO are conserved among kingdoms more strongly than are primary or quaternary structures.

What advantage might there be to an organism of an altered quaternary structure in an enzyme that preserves its tertiary fold? The most obvious answer is that a preserved tertiary structure maintains a useful catalytic function, whereas an altered quaternary structure presents new opportunities for regulation. In RuBisCO, the tetramerized L_2 structure of the plant enzyme permits interaction of the four L_2 pairs, perhaps mediated by the S subunits that appear to act as a scaffold for the L_2 pairs. In the hypothetical higher GS structure of Figure 5, the 8 open "half-active sites" could conceivably function in the octamer as regulatory sites. Each putative regulatory half site belongs to the same subunit as part of a full active site; consequently, the binding of an effector could be communicated to the catalytic center through the subunit.

Testing of these speculative notions must await more detailed comparison of RuBisCO structures, as well as the determination of the structure of higher cell GS.

ACKNOWLEDGMENTS

The authors gratefully acknowledge support from the National Institutes of Health research (United States Public Health Service GM-31299).

REFERENCES

Almassy, R.J., C.A. Janson, R. Hamlin, N.-H. Xuong, and D. Eisenberg. 1986. Novel subunit-subunit interactions in the structure of glutamine synthetase. *Nature* **323:** 304.

Baker, T.S., D. Eisenberg, F.A. Eiserling, and L. Weissman. 1975. The structure of form I crystals of D-ribulose-1,5-diphosphate carboxylase. *J. Mol. Biol.* **91:** 391.

Banner, D.W., A.C. Bloomer, G.A. Petsko, D.C. Phillips, C.I. Pogson, and I.A. Wilson. 1975. Structure of chicken muscle triose phosphate isomerase determined crystallographically. *Nature* **255:** 609.

Chapman, M.S., S.W. Suh, D. Cascio, W.W. Smith, and D. Eisenberg. 1987. The quaternary structure of plant RuBisCO limits sliding-layer conformational change. *Nature* (in press).

Chapman, M.S., W.W. Smith, S.W. Suh, D. Cascio, A. Howard, R. Hamlin, N.-H. Xuong, and D. Eisenberg. 1986. Structural studies of RuBisCO from tobacco. *Philos. Trans. R. Soc. Lond. B Biol. Sci.* **313:** 367.

Colombo, G. and J.J. Villafranca. 1986. Amino acid sequence of *Escherichia coli* glutamine synthetase deduced from the DNA nucleotide sequence. *J. Biol. Chem.* **261:** 10587.

Ellis, R.J. and J.C. Gray, eds. 1986. *Ribulose bisphosphate carboxylase-oxygenase.* The Royal Society, London.

Ginsburg, A. 1972. Glutamine synthetase of *Escherichia coli*: Some physical and chemical properties. *Adv. Protein Chem.* **26:** 1.

Ginsburg, A. and E.R. Stadtman. 1973. Regulation of glutamine synthetase in *Escherichia coli*. In *The enzymes of glutamine metabolism* (ed. S. Prusiner and E.R. Stadtman), p. 92. Academic Press, New York.

Hayward, B.E., A. Hussain, R.H. Wilson, A. Lyons, V. Woodcock, B. McIntosh, and T.J.R. Harris. 1986. The cloning and nucleotide sequence of cDNA for an amplified glutamine synthetase gene from the Chinese hamster. *Nucleic Acids Res.* **14:** 999.

Janson, C.A., W.W. Smith, and D. Eisenberg. 1984. Preliminary structural studies of ribulose-1,5-bisphosphate carboxylase/oxygenase from *Rhodospirillum rubrum*. *J. Biol. Chem.* **259:** 11594.

Janson, C.A., P.S. Kayne, R.J. Almassy, M. Grunstein, and D. Eisenberg. 1986. DNA-encoded sequence of glutamine synthetase from *Salmonella typhimurium*: Implications for the protein structure. *Gene* **46:** 297.

Maurizi, M.R., H.B. Pinkofsky, P.J. McFarland, and A. Ginsburg. 1986. Mg^{2+} is bound to glutamine synthetase extracted from bovine or ovine brain in the presence of L-methionine-S-sulfoximine phosphate. *Arch Biochem. Biophys.* **246:** 494.

McFadden, B.A., J. Torres-Ruiz, H. Daniell, and G. Sarojini. 1986. Interaction, functional relations and evolution of large and small subunits in RuBisCO from prokaryota and eukaryota. *Philos. Trans. R. Soc. Lond. B Biol. Sci.* **313:** 347.

Meister, A. 1974. Glutamine synthetase of mammals. In *The enzymes*, 3rd. edition (ed. P.D. Boyer), vol. 10, p.10. Academic Press, New York.

Miziorko, H.M. and G.H. Lorimer. 1983. Ribulose-1,5-bisphosphate carboxylase/oxygenase. *Annu. Rev. Biochem.* **52:** 507.

Schneider, G., Y. Lindqvist, C.-I. Branden, and G. Lorimer. 1986. Three-dimensional structure of ribulose-1,5-bisphosphate carboxylase/oxygenase from *Rhodospirillum rubrum* at 2.9 Å resolution. *EMBO J.* **5:** 3409.

Shapiro, B.M., H.S. Kingdon, and E.R. Stadtman. 1967. Adenylylglutamine synthetase: A new form of the enzyme with altered regulatory and kinetic properties. *Proc. Natl. Acad. Sci.* **58:** 642.

Sweet, R.M. and D. Eisenberg. 1983. Correlation of sequence hydrophobicities measures similarity in three-dimensional protein structure. *J. Mol. Biol.* **171:** 479.

Tate, S.S. and A. Meister. 1971. Regulation of rat liver glutamine synthetase: Activation by α-ketoglutarate and inhibition by glycine, alanine, and carbamyl phosphate. *Proc. Natl. Acad. Sci.* **68:** 781.

———.1973. Glutamine synthetases of mammalian liver and brain. In *The enzymes of glutamine metabolism* (ed. S. Prusiner and E.R. Stadtman), p. 77. Academic Press, New York.

Tate, S.S., L. Fang-Yun and A. Meister. 1972. Rat liver glutamine synthetase. *J. Biol. Chem.* **247:** 5312.

Tischer, E., S. DasSarma, and H.M. Goodman. 1986. Nucleotide sequence of an alfalfa glutamine synthetase gene. *Mol. Gen. Genet.* **203:** 221.

Tumer, N.E., S.J. Robinson, and R. Haselkorn. 1983. Different promoters for *Anabaena* glutamine synthetase gene during growth using molecular or fixed nitrogen. *Nature* **306:** 337.

Wedler, F.C., R.B. Denman, and W.G. Roby. 1982. Glutamine synthetase from ovine brain is a manganese(II) enzyme. *Biochemistry* **21:** 6389.